Theoretical studies of the effects of matrix composition, lattice temperature, and isotopic substitution on isomerization reactions of matrixisolated HONO/Ar

Paras M. Agrawal, Donald L. Thompson, and Lionel M. Raff

Citation: The Journal of Chemical Physics **102**, 7000 (1995); doi: 10.1063/1.469093
View online: http://dx.doi.org/10.1063/1.469093
View Table of Contents: http://scitation.aip.org/content/aip/journal/jcp/102/18?ver=pdfcov
Published by the AIP Publishing

Theoretical studies of the effects of matrix composition, lattice temperature, and isotopic substitution on isomerization reactions of matrix-isolated HONO/Ar

Paras M. Agrawal, Donald L. Thompson, and Lionel M. Raff
Department of Chemistry, Oklahoma State University, Stillwater, Oklahoma 74078

(Received 26 September 1994; accepted 1 February 1995)

Theoretical molecular dynamics studies of matrix composition, lattice temperature, and isotopic substitution effects upon *cis–trans* isomerization rates and the vibrational relaxation rates to lattice phonon modes of matrix-isolated HONO, DONO, and $H^{18}ON^{18}O$ systems are reported. The results show that isomerization is usually slower in an argon matrix than in xenon. The calculated ratios of the rates for different initial vibrational energy distributions correlate well with the ratio of the well-depth parameters for the lattice/HONO interactions. In all cases examined, the matrix-isolated isomerization rate is enhanced relative to the gas-phase rate. This behavior is attributed to a vibration → lattice phonon modes → rotation → torsional vibration) isomerization mechanism. Isomerization in both Xe and Ar matrices is nonstatistical with pronounced mode specificity present in both environments. In the gas phase, deuterium and ^{18}O substitution produce small, positive enhancements of the isomerization rate by 13% and 26%, respectively, due to an increased kinetic coupling to the torsional modes. In the matrix, however, the isotope effects are negative and larger in magnitude. This reversal is attributed to a reduced rate of energy transfer from the lattice to rotation of DONO and $H^{18}ON^{18}O$ due to the increased moment of inertia. In general, all of the present results support a matrix HONO isomerization mechanism via a (vibration→lattice phonon modes →rotation→torsional vibration) energy transfer pathway.

I. INTRODUCTION

We have previously reported a series of theoretical studies of several aspects of the mode selective isomerization dynamics of HONO in the gas phase.[1–6] Recently, these investigations have been extended to the matrix-isolated HONO/Xe system.[7] In this study molecular dynamics simulations were employed to examine *cis–trans* isomerization reactions, intramolecular vibration relaxation (IVR), and vibrational relaxation rates to lattice phonon modes of HONO isolated in a face-centered cubic (fcc) xenon matrix at 12 K. It is found that both *cis→trans* and *trans→cis* isomerization rates are significantly enhanced over the corresponding gas-phase values by the presence of the matrix in spite of the steric effects produced by the environment. This result occurs because the matrix opens a (vibration→lattice phonon modes→rotation→torsional vibration) energy transfer path. The calculated isomerization rate coefficients indicate the presence of significant nonstatistical dynamics. The IVR rates in the matrix and in the gas phase are slow relative to the isomerization rates. Consequently, isomerization cannot be statistical. The calculated *cis→trans* to *trans→cis* ratio is found to be significantly less than previously reported measurements indicate.

Our previous results[7] show that vibrational relaxation rates to the lattice phonon modes are almost independent of the initial energy partitioning. This result led us to suggest that the transfer rates may be approaching the limiting values determined by the Debye frequency of the lattice.

By carrying out analogous computations in the presence of lattice vacancies, we found that the presence of such vacancies exerts a profound influence upon the dynamics. When the percentage of lattice vacancies approaches 20%, the calculated dynamics in the matrix approach the gas-phase results.[7]

The present paper reports the results of extended investigations of matrix-isolated HONO systems. In particular, the effects of matrix composition, isotopic substitution, and lattice temperature are examined. The specific systems studied include HONO, DONO, and $H^{18}ON^{18}O$ in Xe and Ar matrices at 4, 12, and 40 K.

II. MATRIX MODEL, POTENTIAL ENERGY SURFACE AND NUMERICAL METHODS

The model employed for the rare-gas matrix is the same as that used in our earlier investigations.[7,8] The matrix is simulated by a $5\times5\times5$ face-centered cubic (fcc) lattice consisting of 125 unit cells having 666 atoms. Either HONO, DONO, or $H^{18}ON^{18}O$ is placed inside the matrix such that its center of mass coincides with the center of mass of the isolated lattice.

The total potential is the same as that used in Ref. 7. It consists of the sum of three terms,

$$V = V_m + V_i + V_h , \tag{1}$$

where V_m is the rare-gas/rare-gas potential, V_h is the intramolecular potential for HONO in the absence of the matrix, and V_i gives the interaction between the atoms of HONO and those of the lattice.

The V_h potential is that previously employed by Chambers and Thompson.[2] It comprises three bond stretching terms which are taken as Morse functions, two harmonic bending terms, and one cosine series of the dihedral angle to

 0021-9606/95/102(18)/7000/6/$6.00

TABLE I. Pairwise potential parameters for an argon lattice. D and ϵ are in eV. r and σ are in Å. α is in $Å^{-1}$.

Pair	D or ϵ	α	r or σ
Ar–Ar	0.012 228 90	1.745	3.810
Ar–O	0.005 379 80		3.273
Ar–N	0.004 839 14		3.466
Ar–H	0.001 571 85		3.526

account for torsional effects. The potential uses attenuation terms to smoothly switch between the *cis* and *trans* geometries. It has been shown[2] that this potential yields very good results for the predicted HONO geometry, energetics, and normal-mode frequencies.

Both V_m and V_i are assumed to have pairwise form. The functional forms are taken to be Morse functions for V_m and Lennard-Jones (12,6) potentials for V_i. These are described in more detail in Ref. 7. The potential parameters for these terms are given in Ref. 7 for the Xe lattice and in Table I for an Ar matrix. The mixed interactions have been obtained using standard combination rules, arithmetic mean for the equilibrium distances and geometric mean for the well depth, together with literature data for the pure systems.[8–11]

Quasiclassical trajectories are calculated by integrating the equations of motion for all atoms except the boundary atoms of the lattice. A fourth-order Runge–Kutta method is used with a step size of 0.195 556 fs. Energy dissipation to the bulk of the lattice not explicitly included in the 666-atom model is incorporated using the velocity reset method developed by Riley, Coltrin, and Diestler[12] together with the parameters given in Ref. 10.

In addition to zero-point energy, one or more normal modes, as specified in Table II, are assigned a few quanta of vibrational excitation energy. In the notation $(n_1, n_2, n_3, n_4, n_5, 0)$ used in this paper to specify the initial vibrational state of HONO, the value of n_i is such that $(n_i+0.5)h\nu_i$ gives the initial vibrational energy of the ith vibrational normal mode, where h is Planck's constant and ν_i is the vibrational frequency corresponding to mode i. The subscript $i=1,2,3,4,5,6$ denotes the O–H stretch, the N═O stretch, the HON bend, the O–N stretch, the ONO bend, and the torsional mode, respectively. Vibrational phase averaging is achieved using the procedures described in Ref. 7.

TABLE II. Computed *cis*→*trans* isomerization rate coefficients and rate coefficients for energy transfer to the Ar lattice phonon modes.

Molecule	Mode	Lattice temp. (K)	Isomerization rate $k(ps^{-1})$ Lattice	Gas phase	R_x	E transfer $k_v(ps^{-1})$ non-R_x
HONO	(1,2,3,4,5,0)	12	0.98	0.72	0.18	0.031
	(3,0,0,0,0,0)	12	0.86	0.23	0.15	0.030
	(0,6,0,0,0,0)	12	0.38	0.15	0.10	0.013
	(0,0,8,0,0,0)	12	2.62	2.11	0.14	0.028
	(0,0,0,10,0,0)	12	0.53	0.27	0.14	0.057
	(0,0,0,0,16,0)	12	0.32	0.20	0.12	0.033
HONO	(0,6,0,0,0,0)	4	0.30	0.15	0.12	0.016
	(0,6,0,0,0,0)	40	0.42	0.19	0.12	0.016
DONO	(0,6,0,0,0,0)	12	0.26	0.17	0.06	0.006
$H^{18}ON^{18}O$	(0,6,0,0,0,0)	12	0.29	0.19	0.13	0.016

In all cases, the initial rotational energy of HONO is taken to be zero. Random orientation of HONO relative to the lattice atoms is achieved by random rotation about each of its three principal axes. A damped trajectory method, described in Ref. 7, is used to relax the HONO/matrix system to its nearest local potential minimum. Subsequently, the lattice atoms are given energy in accord with the desired lattice temperature, T, by assignment of a momentum equal to $\pm[2mk_bT]^{0.5}$ to each momentum component, where m is the lattice–atom mass and k_b is Boltzmann's constant. The direction of the momentum component is chosen randomly with equal probability.

During the numerical integration, the boundary atoms (B zone) are held fixed. Consequently, the minimum potential states to which the damped trajectory procedure relaxes the system are states at constant (T,V) rather than states at constant (T,P) as is the case for most matrix experiments. However, we have previously shown[8] that the volume expansion of the local environment produced by matrix isolation of 1,2-difluoroethane decreases with increasing radial distance and becomes vanishing small beyond a radial distance of 10 Å measured from the center of the innermost unit cell of the lattice. With HONO, the effect will be even smaller. Consequently, the volume change of the crystal produced by the presence of HONO is negligible. Under these conditions, we expect that the minimum potential states and the dynamics of the constant (T,V) matrix model will adequately represent the actual experiment, which is conducted under constant (T,P) conditions. We also note here that because of the low temperature and very small changes in entropy and volume upon isomerization, the minimum potential-energy pathway is expected to be nearly identical to the minimum Helmholtz and Gibbs energy pathways.

Isomerization is defined in terms of the HONO dihedral angle, ϕ. The equilibrium *cis* conformation has $\phi=0°$, whereas the *trans* isomer has $\phi=180°$ at equilibrium. *cis*→*trans* isomerization is defined to have occurred whenever the dihedral angle for a *cis* conformation changes such that ϕ falls in the range $170°\leqslant\phi\leqslant180°$. When this occurs, the reaction time is taken to be the time at the crossing of the barrier crest, which occurs at $\phi=85°$. For *trans*→*cis* isomerization, reaction is considered to have occurred whenever ϕ is found to lie in the range $0°\leqslant\phi\leqslant10°$. In this case, the reaction time is again taken to be the time of barrier crossing.

Isomerization rate coefficients for HONO, DONO, and $H^{18}ON^{18}O$ are obtained from a first-order exponential decay equation

$$N=N_0\ \exp[-kt], \tag{2}$$

where N_0 is the total number of trajectories computed and N is the number of unisomerized trajectories at time t. If Eq. (2) is found to accurately describe the decay dynamics, the slope of a plot of $\ln[N/N_0]$ vs time will be $-k$. Typical results are shown in Fig. 1.

We have previously noted[7] that HONO vibrational en-

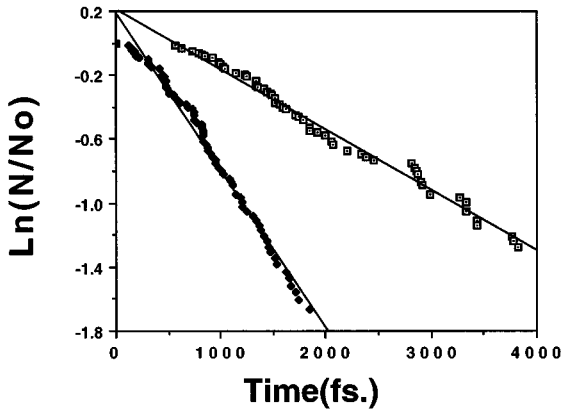

FIG. 1. Logarithmic decay plots for *cis→trans* isomerization of HONO in an Ar matrix at 12 K with 1.7 eV of internal energy. The lines are least-squares fits. The open rectangles correspond to a (0,6,0,0,0,0) initial vibrational energy distribution as defined in the text. The solid rectangles are for a (1,2,3,4,5,0) initial vibrational energy distribution.

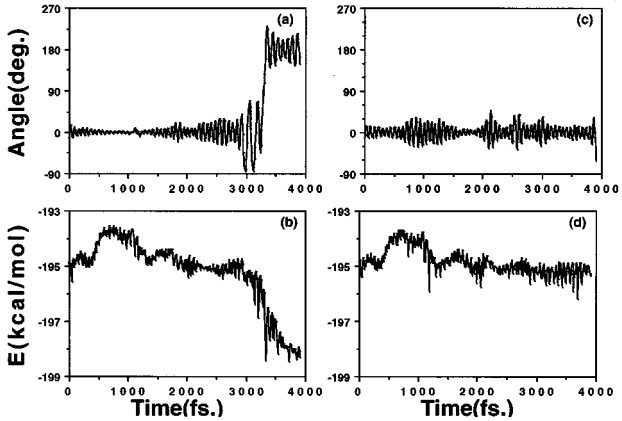

FIG. 3. (a) The variation of the DONO dihedral angle as a function of time for a trajectory undergoing *cis→trans* isomerization. The initial energy distribution is (0,6,0,0,0,0). (b) The corresponding variation of DONO internal energy. The energy zero corresponds to the energy of totally dissociated DONO with all atoms at rest. (c) and (d) are the same as (a) and (b), respectively, for a nonreactive trajectory of DONO.

ergy transfer to the phonon of a Xe lattice follows a first-rate rate law of the form

$$\frac{dE_v}{dt} = -k_v[E_v - E_{\mathrm{eq}}], \tag{3}$$

where E_v is the HONO vibrational energy which is taken to be the HONO kinetic energy plus V_h, E_{eq} is the value of E_v when HONO is in thermal equilibrium with the lattice, and K_v is the characteristic energy transfer rate coefficient. Since $E_v \gg E_{\mathrm{eq}}$ in the present cases, Eq. (3) predicts a simple exponential decay of the internal HONO vibrational energy with a rate coefficient k_v. The same type of first-order behavior is observed in an argon matrix. Figure 2 shows the variation of $\log(E_v/E_0)$ as a function of time, where E_0 is the initial value of E_v, in an Ar lattice with HONO initially in the (0,6,0,0,0,0) vibrational state. The near linearity of the plots for both reactive and nonreactive trajectories is evident. The faster energy transfer rate for the reactive trajectories is similar to that obtained for a Xe matrix.[7] This is a reflection of the fact that the transfer rate from the HONO torsional mode to the phonon modes of the lattice is very large.

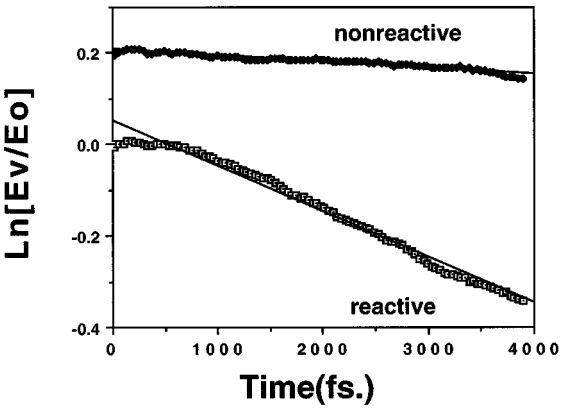

FIG. 2. Logrithmic decay plots for the ratio of the average HONO internal energy to its initial value. The open rectangles represent the data for reactive trajectories. The solid rectangles denote the data for trajectories not undergoing isomerization. The lines are linear least-squares fits. The initial vibrational state is (0,6,0,0,0,0). For visualization clarity, the ordinate value for the nonreactive trajectories is increased by 0.2 at all points.

The efficiency of energy transfer between the DONO torsional mode and the lattice can also be seen by comparing two typical trajectories, one undergoing isomerization and a second not isomerizing. Figures 3(a) and 3(c) show the time variation of the DONO dihedral angle. Figure 3(a) indicates that isomerization takes place around 3300 fs for this trajectory whereas Fig. 3(b) shows that particular trajectory to be unreactive. The time variation of E_v for the two trajectories are given in Figs. 3(b) and 3(d), respectively. The rapid decrease of E_v seen in Fig. 3(b) in the interval of time around 3300 fs is typical of a reactive trajectory in which a relatively large torsional energy is rapidly transferred to the lattice modes. Such a rapid decrease in E_v is not seen in Fig. 3(d) since this trajectory does not isomerize and hence, never attains a large energy in the DONO torsional mode.

The effect of matrix composition and lattice temperature upon the isomerization rate is determined by computing the isomerization rate for HONO initially in the (0,6,0,0,0,0) vibrational state in Xe and Ar lattices at 4, 12, and 40 K. The mode specificity of the isomerization process is investigated for HONO by computation of the rate for different initial vibrational state assignments each with nearly identical total internal energy. Isotope effects for deuterium and ^{18}O substitution are explored by computation of the isomerization rates for the same vibrational energy distribution, (0,6,0,0,0,0), with the total energy scaled to 1.7 eV. The maximum integration time corresponds to 5.8 ps. The results of all calculations are summarized in Table II.

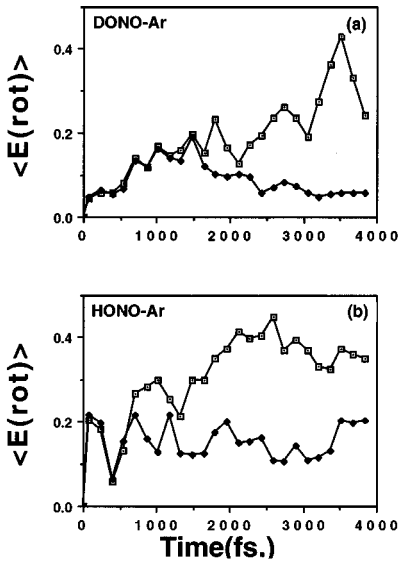

FIG. 4. Average rotational energy of (a) DONO and (b) HONO in kcal/mol as a function of time. Open rectangles correspond to the average over trajectories undergoing isomerization. Solid rectangles represent the results for nonreactive trajectories. The initial vibrational state is (0,6,0,0,0,0).

III. DISCUSSION

A. Effects of matrix composition

In almost all cases, the energy transfer rates to the lattice phonon modes are lower in an argon matrix than is the case for xenon. Using data given in Table II and Ref. 7, we find that at a constant temperature of 12 K, the computed $[k_v]_{Ar}/[k_v]_{Xe}$ ratios all lie in the range 0.37 to 1.06 with most of the values around 0.72. Since the ratio of the well depth parameters, $[\epsilon(Ar–X)]/[\epsilon(Xe–X)]$ with X=O, N, or H, is 0.71, it appears that the difference in energy transfer rates to the lattice is a reflection of differences in the magnitude of the interaction forces.

The reduced interaction forces in an Ar matrix relative to those present in Xe also result in a reduced rate for energy transfer from the lattice phonon modes to rotation of HONO. Figure 4 shows the average rotational energy transferred to DONO and HONO for reactive and nonreactive trajectories in an argon lattice. Comparison of Fig. 4(b) with the corresponding results for a Xe lattice, Fig. 2 of Ref. 7, shows that the rate of transfer of energy from the lattice to HONO rotation is approximately three times greater in Xe than in Ar.

In all cases studied, the matrix-isolated isomerization rate is enhanced relative to the gas-phase rate. The data given in Table II show that the magnitude of the enhancement depends on the initial mode of vibration excited, the temperature of the lattice, and the isotopic mass. This behavior is not unexpected as similar effects were observed in our initial studies of matrix-isolated HONO isomerization.[7] We have previously attributed these effects to a (vibration→lattice phonon modes→rotation→torsional vibration) energy transfer path.[7] Since the first two steps of this mechanism involving energy transfer to and from the lattice phonon modes are slowed in the argon matrix relative to their values in xenon, we would expect the corresponding isomerization rates for the same initial energy partitioning and lattice temperature to also be depressed. The data show this to be the case. The data reported in Table III further indicate that there is a good quantitative correlation between the computed $[k_v]_{Ar}/[k_v]_{Xe}$ ratios and the corresponding ones for $[k]_{Ar}/[k]_{Xe}$. The present results are therefore consistent with our previously suggested[7] isomerization mechanism.

TABLE III. Correlation between k_{Ar}/k_{Xe} and $[k_v]_{Ar}/[k_v]_{Xe}$ for matrix-isolated HONO.

Initial state	k_{Ar}/k_{Xe}	$[k_v]_{Ar}/[k_v]_{Xe}$
(1,2,3,4,5,0)	1.03	1.05
(0,0,8,0,0,0)	0.97	0.78
(0,6,0,0,0,0)	0.72	0.71

The data reported in Table II show that the isomerization rate increases with an increase of the lattice temperature. This is the expected effect since an increase of lattice temperature enhances the rate of the step involving energy transfer from the lattice phonon modes to rotation of HONO. However, it should be noted that the temperature effect is small. A tenfold increase of lattice temperature from 4 to 40 K produces only a 40% increase in the isomerization rate. This behavior is not surprising in view of the very high initial energy of HONO compared to the thermal energy of the lattice. The lack of sensitivity of the isomerization rate to the lattice temperature in laser excitation experiments has been previously been reported by McDonald and Shirk[13] and by Shirk and Shirk.[14]

We have previously noted[7] that the gas-phase intramolecular energy transfer rates between different vibrational modes of HONO are lower than the isomerization rate. Consequently, gas-phase isomerization of HONO is a nonstatistical process which exhibits pronounced mode specificity. When HONO is matrix isolated in either Xe or Ar, intramolecular energy transfer to the torsional mode is accelerated due to the coupling among the different vibrational modes and the lattice. As a result, the isomerization rates in the matrix environment exceed those for the gas phase. However, as the data given in Table II show, the energy transfer rate coefficients, k_v, are still low relative to the rate coefficients for isomerization. Consequently, mode specificity and nonstatistical dynamics remain.

The acceleration effect due to HONO/lattice coupling is also mode dependent and this dependency is a function of the lattice composition. For example, the data given in Ref. 7 and Table II indicate that the HON bending is very effectively coupled to the torsional mode even in the gas phase. As a result, the additional coupling provided by the lattice is of minor importance and the acceleration of the isomerization rate is only about 25%–28% in both Ar and Xe matrices when the excitation energy is initially in the HON bend. In contrast, the coupling between the ONO bend and the torsion modes does not provide an effective energy transfer pathway in the gas phase. Hence, the matrix environment exerts a much more pronounced accelerating effect on the isomerization rate. In a Xe matrix, the acceleration is 195% for an

initial (0,0,0,0,16,0) energy partitioning,[7] but in Ar with a much weaker HONO/lattice coupling, the acceleration is only 60%.

B. Isotope effects

The Ar matrix-isolated results for HONO, DONO, and $H^{18}ON^{18}O$ indicate the presence of significant isotope effects. In contrast, in the gas phase for an initial (0,6,0,0,0,0) energy partitioning, there is only a small positive effect. That is, the calculated isomerization rates for DONO and $H^{18}ON^{18}O$ are larger than that for HONO by 13% and 26%, respectively. We interpret this to be due to an increase in the kinetic coupling terms between the N═O stretch and torsional modes for the heavier isotopes. In the argon matrix, however, the isotope effects are negative, i.e., the isomerization rate for HONO/Ar is larger than those for DONO/Ar and $H^{18}ON^{18}O$/Ar by 32% and 24%, respectively.

From the point of view of isomerization rate enhancement by the Ar matrix, we find $[k(\text{HONO/Ar})/k(\text{HONO})]$ to be 2.53 whereas $[k(\text{DONO/Ar})/k(\text{DONO})]$ and $[k(H^{18}ON^{18}O/\text{Ar})/k(H^{18}ON^{18}O)]$ are only 1.53. Thus the matrix environment is significantly more effective in enhancing isomerization of HONO than is the case for isotopically substituted molecules. Qualitatively similar experimental trends for these molecules in an N_2 matrix have been reported by Pimentel and co-workers.[15,16]

We interpret the observed isotope effects to be due primarily to a difference in the magnitude of the second step in the general (vibration→lattice phonon modes→rotation →torsional vibration) mechanism for the process. Figure 4 shows the average rotational energy in reactive and nonreactive trajectories for HONO/Ar and DONO/Ar systems. In the first 2 ps, the average gain of rotational energy by reacting HONO molecules is 0.37 kcal/mol compared to 0.27 kcal/mol for DONO. Similar studies on $H^{18}ON^{18}O$ show that its average rotational energy over this time interval is about 0.29 kcal/mol. As a result of this faster second step, the matrix enhances the isomerization rate of HONO much more than is the case for DONO or $H^{18}ON^{18}O$. In the gas phase, this factor is eliminated and the only relevant consideration is the increased kinetic coupling between the N═O stretch and torsional modes. Since we expect for a given value of the exerted torque, the rate of gain of rotational energy from the lattice phonon modes to decrease with an increase of the moment of inertia of the molecule, the observed qualitative trends are those which would be expected if the overall process is correctly described by the (vibration→lattice phonon modes→rotation→torsional vibration) mechanism.

IV. SUMMARY

Theoretical molecular dynamics studies of matrix composition, lattice temperature, and isotopic substitution effects upon *cis–trans* isomerization rates and the vibrational relaxation rates to lattice phonon modes of matrix-isolated HONO, DONO, and $H^{18}ON^{18}O$ systems are reported. These studies are an extension of our previous investigation of statistical/nonstatistical behavior and the effects of the matrix environment and lattice imperfections in the HONO/Xe system.[7]

We find that isomerization is usually slower in an argon matrix than in xenon. The calculated ratios of the rates for different initial vibrational energy distributions correlate well with the ratio of the well-depth parameters for the lattice/HONO interactions. The rate differences therefore appear to be due primarily to differences in the interaction forces rather than the unit cell spacing in Ar and Xe matrices.

In all cases examined, the matrix-isolated isomerization rate is enhanced relative to the gas-phase rate. We have previously[7] attributed this behavior to a (vibration→lattice phonon modes→rotation→torsional vibration) energy transfer mechanism which is absent in the gas phase. The present calculations support this interpretation. The smaller interaction forces present in an Ar lattice decrease the rate of the two energy transfer steps. Consequently, the matrix enhancement of the isomerization rate is less in Ar than in Xe. Analysis of the data shows that a good correlation exists between the ratio of the isomerization rates in Ar and Xe and the corresponding ratio of rates for energy transfer to the lattice modes.

Isomerization in both Xe and Ar matrices is nonstatistical. Pronounced mode specificity is present in both environments.

In the gas phase, deuterium and ^{18}O substitution produce small, positive enhancements of the isomerization rate by 13% and 26%, respectively. In the matrix, however, the isotope effects are negative and larger in magnitude. The reversal is attributed to a reduced rate of energy transfer from the lattice to rotation of DONO and $H^{18}ON^{18}O$ due to the increased moment of inertia. This effect counterbalances the increased kinetic coupling in the isotopically substituted molecules which leads to a small, positive isotope effect in the gas phase. The same effects are responsible for a larger enhancement of the HONO isomerization rate by the matrix compared to the gas phase rate than is observed for either DONO or $H^{18}ON^{18}O$.

In general, all of the present results support our previously suggested mechanism[7] that in a matrix environment, HONO isomerization occurs principally via a (vibration →lattice phonon modes→rotation→torsional vibration) energy transfer mechanism.

ACKNOWLEDGMENTS

We are pleased to acknowledge financial support from the National Science Foundation Grant No. CHE-9211925 and from the Air Force Office of Scientific Research Grant Nos. F49620-92-J-0011 and F49620-93-1-0237. P.M.A. thanks Vikram University, Ujjain, India, for granting him leave to pursue this research.

[1] Y. Qin and D. L. Thompson, J. Chem. Phys. **100**, 6445 (1994).
[2] C. C. Chambers and D. L. Thompson, Chem. Phys. Lett. **218**, 166 (1994).
[3] Y. Qin and D. L. Thompson, J. Chem. Phys. **96**, 1992 (1992).
[4] D. L. Thompson, in *Proceedings 24th Jerusulem Symposium on Quantum Chemistry, Mode Selective Chemistry*, edited by B. Pullman, J. Jortner, and R. D. Levine (Reidel, Dordrecht, 1991), p. 261.
[5] Y. Guan and D. L. Thompson, Chem. Phys. **139**, 147 (1989).

[6] Y. Guan, G. C. Lynch, and D. L. Thompson, J. Chem. Phys. **87**, 6957 (1987).
[7] P. M. Agrawal, D. L. Thompson, and L. M. Raff, J. Chem. Phys. **101**, 9937 (1994).
[8] L. M. Raff, J. Chem. Phys. **93**, 3160 (1990).
[9] M. B. Ford, A. D. Foxworthy, G. J. Mains, and L. M. Raff, J. Phys. Chem. **97**, 12134 (1993).
[10] L. M. Raff, J. Chem. Phys. **95**, 8901 (1991).
[11] R. Gunde, P. Felder, and Hs. H. Gunthard, Chem. Phys. **64**, 313 (1982).
[12] M. E. Riley, M. E. Coltrin, and D. J. Diestler, J. Chem. Phys. **88**, 5934 (1988).
[13] P. A. McDonald and J. S. Shirk, J. Chem. Phys. **77**, 2355 (1982).
[14] A. E. Shirk and J. S. Shirk, Chem. Phys. Lett. **97**, 549 (1983).
[15] R. T. Hall and G. C. Pimentel, J. Chem. Phys. **38**, 1889 (1963).
[16] J. D. Baldeschwieler and G. C. Pimentel, J. Chem. Phys. **33**, 1008 (1960).